On the use of an absorption layer for the angular spectrum approach (L)

Yun Jing

Citation: The Journal of the Acoustical Society of America **131**, 999 (2012); doi: 10.1121/1.3675967
View online: https://doi.org/10.1121/1.3675967
View Table of Contents: https://asa.scitation.org/toc/jas/131/2
Published by the Acoustical Society of America

LETTERS TO THE EDITOR

This Letters section is for publishing (a) brief acoustical research or applied acoustical reports, (b) comments on articles or letters previously published in this Journal, and (c) a reply by the article author to criticism by the Letter author in (b). Extensive reports should be submitted as articles, not in a letter series. Letters are peer-reviewed on the same basis as articles, but usually require less review time before acceptance. Letters cannot exceed four printed pages (approximately 3000–4000 words) including figures, tables, references, and a required abstract of about 100 words.

On the use of an absorption layer for the angular spectrum approach (L)

Yun Jing[a)]
Department of Mechanical and Aerospace Engineering, North Carolina State University, Raleigh, North Carolina 27695

(Received 22 August 2011; revised 30 November 2011; accepted 16 December 2011)

Reducing the spatial aliasing error of the angular spectrum method by using an absorption layer is investigated in this paper. The acoustic equation including the absorption layer is presented and is transformed in the spatial frequency domain, where an implicit analytic solution is readily available. Its approximation, which is more suitable for numerical simulation, is derived and is numerically implemented. The comparisons between the present method and available methods demonstrate its validity and advantages. © *2012 Acoustical Society of America*. [DOI: 10.1121/1.3675967]

PACS number(s): 43.35.Bf, 43.20.Bi [TDM] Pages: 999–1002

I. INTRODUCTION

Angular spectrum approach (ASA) has been widely used to analyze and predict the acoustic field from a transducer.[1–5] This approach is considered highly efficient due to its use of the fast Fourier transform (FFT). In addition, since the method only requires two nodes per wavelength to satisfy the Nyquist frequency, the computational burden can be very little compared with other methods.

Two approaches are common for the ASA. The first one directly samples an impulse function and is called the spatially sampled convolution (SSC) algorithm.[1] The second one samples a transfer function, which is the Fourier transform of the impulse function in the spatial frequency domain. It is therefore called the frequency sampled convolution (FSC) algorithm.[1] This study focuses on the FSC algorithm.

The FSC algorithm suffers from the spatial aliasing error.[6,7] In other words, when modeling a transducer using the ASA, instead of a single transducer, infinite sets of transducers are actually modeled. If the computational spatial domain is set to be small, i.e., the distance between each transducers is small, the interference between these transducers will severely distort the acoustic field. Frequency truncation methods were proposed to deal with this type of error.[1,8] In particular, Wu *et al.*[8] proposed applying a spatial frequency low-pass filter to the transfer function, in order to reduce the spatial aliasing error without increasing the computational spatial domain. However, this method has been found to be suboptimal.[5] For radially symmetric sources, wraparound error can be greatly reduced using the ray theory truncation.[1] However, it is found to be not suitable for non-axisymmetric sources.[4] Finally, it is also claimed that the aliasing error can be reduced by applying a window-function to the solution at regular intervals, thus tapering the solution to zero at the edges.[9] This method will be referred to as the tapering method throughout the paper. To the best of our knowledge, the accuracy of the tapering method has not been evaluated so far.

This paper proposes the use of an absorption layer on the boundary of the computational domain to reduce the spatial aliasing error. Even though the same idea has been used in the *k*-space method to reduce the artificial wraparound problems,[10] it cannot be simply duplicated in the ASA, since ASA typically requires a homogeneous acoustic media. In this study, an analytic solution is presented for the case where the attenuation in the media is inhomogeneous, i.e., strong attenuation near the boundary and negligible attenuation away from the boundary. Numerical simulations will be shown. This method will be compared with the tapering method and the SSC algorithm for a square transducer.

II. THEORY

The linearized acoustic wave equation in a homogeneous medium can be written as

$$\left(\nabla^2 - \frac{1}{c_0^2}\frac{\partial^2}{\partial t^2}\right)p(r,t) = 0, \tag{1}$$

where p is the sound pressure and c_0 is the sound speed.

To add the absorption layer on the boundary, a frequency-independent absorption term can be added to Eq. (1),[10–12]

[a)]Author to whom correspondence should be addressed. Electronic mail: yjing2@ncsu.edu

$$\left(\nabla^2 - \frac{1}{c_0^2}\frac{\partial^2}{\partial t^2}\right)p(r,t) = \gamma\frac{\partial p}{\partial t}, \tag{2}$$

where

$$\gamma = \gamma_{\max}/\cosh^2(\alpha n), \tag{3}$$

where $\gamma_{\max}$ is a constant, α is a decay factor, and n denotes the distance in number of grid points from the boundary.[12]

Considering a harmonic case, by Fourier solution the Cartesian x and y dimensions, Eq. (2) is transformed from a partial differential equation to an ordinary differential equation (ODE),

$$\frac{\partial^2 P}{\partial z^2} + K^2 P = F_{xy}(\gamma i\omega p_\omega), \tag{4}$$

where ω is the angular frequency, p_ω represents the pressure amplitude at the frequency ω, P is the Fourier transform of p_ω in terms of x and y, and F_{xy} represents the Fourier transform with regard to Cartesian x and y dimensions. Also we have

$$K^2 = \frac{\omega^2}{c_0^2} - k_x^2 - k_y^2, \tag{5}$$

where k_x and k_y are the wave numbers, $K = +\sqrt{K^2}$, and the frequency ω used here is the negative frequency.

An implicit analytic solution to Eq. (4) can be obtained by using the Green's function and is written as[13]

$$\begin{aligned} P(z) = P(0)e^{iKz} &+ \frac{e^{-iKz}}{2iK}\int_z^{+\infty} e^{iKz'}F dz' - \frac{e^{iKz}}{2iK}\int_z^{+\infty} e^{iKz'}F dz' \\ &+ \frac{e^{iKz}}{2iK}\left[\int_0^z e^{-iKz'}F dz' - \int_0^z e^{iKz'}F dz'\right], \end{aligned} \tag{6}$$

where $F = F_{xy}(\gamma i\omega p_\omega)$.

Equation (6) is not suitable for numerical simulations and needs to be simplified. Since the absorption layer is only supposed to taper the acoustic field very close to the boundary, it can be assumed that the solution approximately equals the solution to the homogeneous equation, i.e., with the right-hand side of Eq. (4) equal to zero. The solution to the homogeneous equation is written as

$$P(z) = P(0)e^{iKz}. \tag{7}$$

Therefore, we have

$$\begin{aligned} F = F_{xy}(\gamma i\omega p_\omega) &= i\omega\Gamma ** P(z) \\ &= i\omega\int \Gamma(\kappa - \kappa')P(z,\kappa')d\kappa' \\ &\approx i\omega\int \Gamma(\kappa - \kappa')P(0,\kappa')e^{iK'z}d\kappa', \end{aligned} \tag{8}$$

where Γ is the Fourier transform of γ, ** denotes convolution, κ is $(k_x, k_y)'$ is the integration variable in the convolution equation, and $K = \sqrt{(\omega/c)^2 - |\kappa|^2}$, $K' = \sqrt{(\omega/c)^2 - |\kappa'|^2}$.

Substituting Eq. (8) into the four integrals in Eq. (6), we have

$$\begin{aligned} &\frac{e^{-iKz}}{2iK}\int_z^{+\infty} e^{iKz'}F dz' - \frac{e^{iKz}}{2iK}\int_z^{+\infty} e^{iKz'}F dz' - \frac{e^{iKz}}{2iK}\int_0^z e^{iKz'}F dz' \\ &\quad\approx -i\omega\frac{e^{iKz}}{2iK}\int\frac{e^{i(K'-K)z} - 1}{i(K+K')}\Gamma(\kappa - \kappa')P(0,\kappa')d\kappa', \end{aligned} \tag{9}$$

where we have assumed that the attenuation is larger than zero [(im$(K) > 0$, so the integration to ∞ converges], but is negligible.

Moveover,

$$\begin{aligned} \frac{e^{iKz}}{2iK}\int_0^z e^{-iKz'}F dz' \approx -i\omega\frac{e^{iKz}}{2iK}\int\frac{e^{i(K'-K)z} - 1}{i(K-K')} \\ \times\Gamma(\kappa - \kappa')P(0,\kappa')d\kappa'. \end{aligned} \tag{10}$$

It is noted that when approaching a one-dimensional problem, where $K' \approx K$, Eq. (10) becomes much larger than Eq. (9), as Eq. (9) approaches zero. For a more general three-dimensional problem, it can be recognized that the difference between Eqs. (9) and (10) comes primarily from $K + K'$ and $K - K'$ in the denominators. For the cases studied here, the former is typically much larger than the latter in directions where the wave energy is significant. For example, when $K' \approx 0$, these two denominators become the same, however, the energy in the direction of $K' \approx 0$, i.e., parallel to the source plane, is very weak, so in this case $P(0, \kappa')$ contributes very little to the integral. Therefore, it is concluded that Eq. (10) can be assumed much larger than Eq. (9) for a general three-dimensional problem. A similar argument was made in a recent study.[13]

Accordingly, the final approximated solution can be written as

$$P(z) \approx P(0)e^{iKz} + \frac{1}{2iK}e^{iKz}\int_0^z e^{-iKz'}F dz', \tag{11}$$

which is in the exact format in a recent study,[13] and can be solved numerically by using the Riemann sums, with a jump step of Δz. The error of the Riemann sums is proportional to the maximum value of the second derivative of the integral function on the interval, and inversely proportional to the square of the number of points on the interval.

It is worth pointing out that, as $\sqrt{k_x^2 + k_y^2}$ approaches k, e^{-iKz} encounters rapidly oscillating real and imaginary components, and numerical calculation of the integral in Eq. (10) requires a fine step size Δz. Nevertheless, for typical transducers, the spatial frequency spectra in that region are quite negligible. Therefore, a low-pass filter can be applied to the spatial frequency domain at every step, so that a large step size can be used.

The acoustic field can be also obtained by[4]

$$p(x,y,z,\omega) = p(x,y,z_0,\omega) ** h(x,y,z - z_0,\omega) \tag{12}$$

and

$$\begin{aligned} h(z,y,z - z_0,\omega) &= \frac{(z - z_0)e^{ikR}}{2\pi R^2}\left(jk - \frac{1}{R}\right), \\ R &= \sqrt{x^2 + y^2 + (z - z_0)^2}. \end{aligned} \tag{13}$$

This is the SSC algorithm. It has been shown that the SSC algorithm is more accurate than the FSC algorithm in an $L \times L$ plane, where $L = D - 2a$, and D is the total length or width of the computational domain, $2a$ is the width of a square transducer.[5]

To close this section, we note that for the tapering method, a tapering function $t(x, y)$ is simply multiplied by the pressure $p(x, y)_\omega$ before being projected by a step size of Δz, thereby immediately yielding a modified angular spectrum of the form

$$P(z + \Delta z) = [P(z) * *T(K)]e^{iK\Delta z}, \tag{14}$$

where T is the Fourier transform of t.

The tapering function in this study is written as[14]

$$t(r) = \begin{cases} 1, & 0 \le r < r_{\max} - r_{\text{wid}} \\ 0.5 \times \{1 + \cos[\pi(r + r_{\text{wid}} - r_{\max})/r_{\text{wid}}]\}, & r_{\max} - r_{\text{wid}} \le r < r_{\max}, \\ 0, & \text{otherwise} \end{cases} \tag{15}$$

where r is the radial distance to the center of the x–y plane, $r_{\max}$ is a half of the total length of x axis or y axis, and r_{wid} is the width of the taper.

III. NUMERICAL SIMULATIONS

To verify the proposed method, a single square piston with the pressure release boundary condition was simulated and the acoustic fields were obtained. The piston had a width of $a = 4$ cm. The excitation signal was a continuous wave at 1 MHz, and the peak pressure was 1 Pa. The speed of sound was 1500 m/s. The maximum transverse extent (the total length of x axis or y axis) was 13.5 cm, which is 90 λ. The sample spacing was a half of the wavelength, i.e., $\lambda/2$. There were 181 points across the x axis and y axis. The step size Δz was λ. For this specific case, an optimized r_{wid} was found to be $r_{\max}/12$ by minimizing the error in the whole computational domain, which will be used in the tapering method. For the present method, the cut-off for the low-pass filter was set at $k_x^2 + k_y^2 = 0.9(\omega^2/c_0^2)$ to allow a large step size Δz. The configuration of the absorption layer was that $\gamma_{\max}$ was 0.5, α was 0.3. It is intuitive that $\gamma_{\max}$ should be set as high as possible to absorb more energy in the absorption layer, however, it is found that larger $\gamma_{\max}$ requires a finer jump step size Δz to keep the algorithm stable. This is because by increasing $\gamma_{\max}$, the inhomogeneous term in Eq. (4) becomes larger, leading to a stiffer ODE that requires a smaller step size. The maximum allowable step size is usually determined by the Lipschitz constant L_1 (Ref. 15) of the inhomogeneous term, and is on the order of $1/L_1$. While L_1 is difficult to be evaluated in Eq. (4), it is found that this configuration of $\gamma_{\max}$ and α is stable for a wide range of cases tested, provided that the step size is smaller or equal to one wavelength.

In addition, up to a certain level, increasing $\gamma_{\max}$ does not significantly change the results. In any case, 0.5 was found to be sufficient for the case tested here. The same rule holds for α. While a small α would absorb more energy and thus reduce the aliasing error, if α was chosen too small, the acoustic field will become inaccurate due to excess absorption. For comparison purposes, a benchmark solution was obtained with a maximum transverse extent of 54 cm using the SSC algorithm.

Figure 1 shows the result along the z axis. The present method agrees with the benchmark solution very well, while the tapering method shows significant errors. The strong oscillations can be reduced by increasing r_{wid}, however, it reduces the accuracy along the transverse dimension. In addition, decreasing the step size Δz does not significantly improve the accuracy for the tapering method. The SSC algorithm was not shown in Fig. 1 because the results overlap with the benchmark solution. Figure 2 shows the results along the transverse direction at a distance of 62.8 cm. The tapering method is again less accurate compared with other methods. The present method becomes significantly inaccurate after about 6 cm while the accuracy of the SSC algorithm drops after 4.75 cm, which corresponds to the prediction[5] $L = D - 2a$. Additional simulations (not presented here) show that the tapering method appears to work well if the computational domain is sufficiently large, e.g., the grid point numbers are 361 in x and y axis in this specific

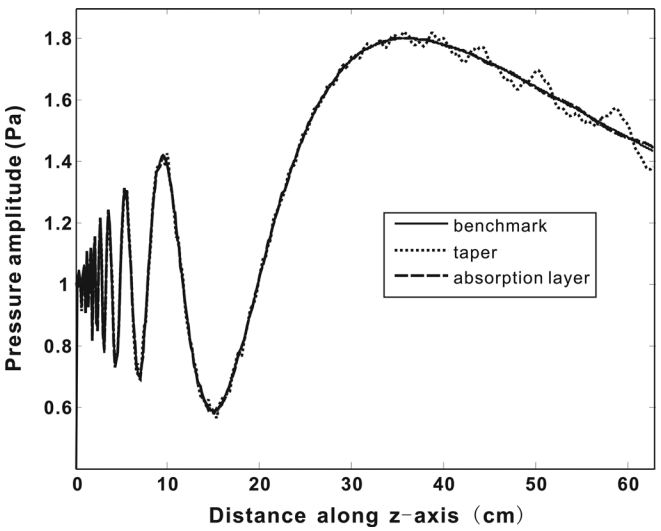

FIG. 1. Simulated pressure distribution of a square piston along the z axis. Results of two different methods (tapering method and the present method) are shown and compared with the benchmark solution.

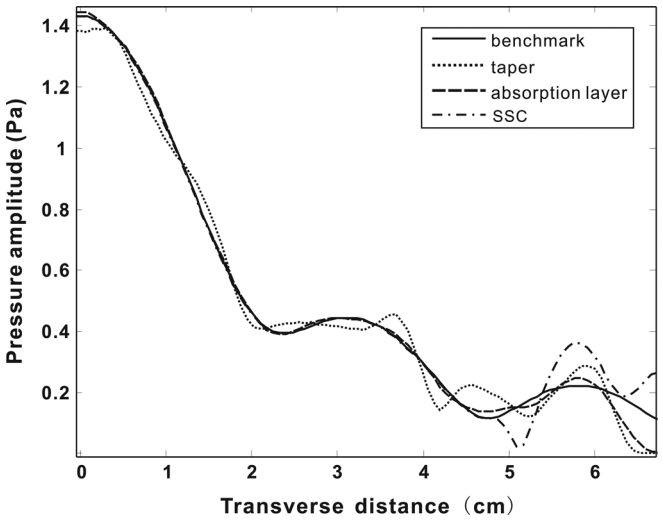

FIG. 2. Simulated pressure distribution of a square piston along the transverse direction at a distance of 62.8 cm. Results of three different methods (tapering method, SSC, and the present method) are shown and compared with the benchmark solution.

case. However, this would also increase the computation time by a factor of 4.

It is worth pointing out that the present method, which is essentially a manipulation of the angular spectrum of the source field, can only result in a reduction of spatial aliasing near the axis of the source if the projected field is made to "roll off" faster than the actual field as a function of distance from the axis. In this way, the tails from the spatial replicas contribute less to the field in the vicinity of the axis than they would otherwise, thereby reducing the appearance of spatial aliasing in that region. This is consistent with Fig. 2, where the computed field is seen to be accurate near the axis of symmetry, while underestimating its amplitude at the outer distance. It is also consistent with the idea of attenuating the field at the boundary of the computational domain.

To quantify the error, the rms mean difference between each method and the benchmark solution was evaluated over the whole volume:

$$\text{error} = \sqrt{\frac{\sum_{x,y,z} \left(p(x,y,z) - p_{\text{exact}}(x,z,y)\right)^2}{\sum_{x,y,z} p_{\text{exact}}(x,z,y)^2}}, \tag{16}$$

and the errors were 0.077, 0.042, and 0.11, for the tapering method, present method, and the SSC algorithm, respectively.

Regarding the computational time, all methods took about the same time as they all require an additional two-dimensional FFT.

IV. CONCLUSIONS

This study proposes the use of an absorption layer to reduce the spatial aliasing error of the ASA method using the FSC algorithm. The acoustic media were considered having extremely strong absorption close to the boundary and negligible absorption elsewhere. An absorption term was added to the acoustic equation, and an implicit analytic solution was proposed that can be solved by the Riemann sums. Numerical simulations were carried out and were compared with the tapering method and the SSC algorithm. It was found that the present method provided more accurate results over the whole computational domain. Since the present method requires projecting the acoustic field step by step with Δz, it can be best used when combining with nonlinear acoustic projection algorithms.[13]

[1]P. T. Christopher and K. J. Parker, "New approaches to the linear propagation of acoustic fields," J. Acoust. Soc. Am. **90**, 507–521 (1991).
[2]P. Wu and T. Stepinski, "Extension of the angular spectrum approach to curved radiators," J. Acoust. Soc. Am. **105**, 2618–2627 (1999).
[3]G. T. Clement and K. Hynynen, "Field characterization of therapeutic ultra-sound phased arrays through forward and backward planar projection," J. Acoust. Soc. Am. **108**, 441–446 (2000).
[4]R. J. Zemp, J. Tavakkoli, and R. S. C. Cobbold, "Modeling of nonlinear ultrasound propagation in tissue from array transducers," J. Acoust. Soc. Am. **113**, 139–152 (2003).
[5]X. Zeng and R. J. McGough, "Evaluation of the angular spectrum approach for simulations of near-field pressures," J. Acoust. Soc. Am. **123**, 68–76 (2008).
[6]P. Wu, R. Kazys, and T. Stepinski, "Analysis of the numerically implemented angular spectrum approach based on the evaluation of two-dimensional acoustic fields. I. Errors due to the discrete Fourier transform and discretization," J. Acoust. Soc. Am. **99**, 1339–1348 (1996).
[7]P. Wu, R. Kazys, and T. Stepinski, "Analysis of the numerically implemented angular spectrum approach based on the evaluation of two-dimensional acoustic fields. II. Characteristics as a function of angular range," J. Acoust. Soc. Am. **99**, 1349–1359 (1996).
[8]P. Wu, R. Kazys, and T. Stepinski, "Optimal selection of parameters for the angular spectrum approach to numerically evaluate acousic field," J. Acoust. Soc. Am. **101**, 125–134 (1997).
[9]T. Varslot and S.-E. Måsøy, "Forward propagation of acoustic pressure pulses in 3D soft biological tissue," Model. Identif. Control **27**, 181–200 (2006).
[10]T. D. Mast, "Two-and three-dimensional simulations of ultrasonic propagation through human breast tissue," ARLO **3**, 53–58 (2002).
[11]A. R. Levander, "Use of the telegraphy equation to improve absorbing boundary efficiency for fourth-order acoustic wave finite difference schemes," Bull. Seismol. Soc. Am. **75**, 1847–1852 (1985).
[12]R. Kosloff and D. Kosloff, "Absorbing boundaries for wave propagation problems," J. Comput. Phys. **63**, 363–376 (1986).
[13]Y. Jing, M. Tao, and G. Clement, "Evaluation of a wave vector frequency domain method for nonlinear wave propagation," J. Acoust. Soc. Am. **129**, 32–46 (2011).
[14]R. C. Waag, J. A. Campbell, J. Ridder, and P. R. Mesdag, "Cross-sectional measurements and extrapolations of ultrasonic fields," IEEE Trans. Ultrason. Ferroelectr. Freq. Control **32**, 26–35 (1985).
[15]T. Donchev and E. Farkhi, "Stability and Euler approximation of one-sided Lipschitz differential inclusions," SIAM J. Control Optim. **36**, 780–796 (1998).